The yearly amount and characteristics of deep-buried phreatic evaporation in hyper-arid areas

Hongshou Li[a, b *], Wanfu Wang[a, b], Hongtao Zhan[b], Fei Qiu[b], Fasi Wu[a, b] and Guobing Zhang[a,b]

[a] *The Conservation Institute of Dunhuang Academy, Dunhuang, 736200, Gansu, China*

[b] *National Ancient Mural Protection Engineering Technology Research Center, Dunhuang, Gansu 736200, China*

Abstract

Water scarcity is the primary cause of land deterioration, so finding new available water resources is crucial to ecological restoration. We investigated a hyper-arid Gobi location in the Dunhuang Mogao Grottoes in this work wherein the burial depth of phreatic water is over 200 m. An air-conditioner was used in a closed greenhouse to condense and measure the yearly amount of phreatic evaporation (PE) from 2010 to 2015. The results show that the annual quantity of PE is 4.52 mm, and that the PE has sinusoidal characteristics. The average PE is 0.0183 mm d^{-1} from March to November. Accordingly, by monitoring the annual changes in soil–air temperature and humidity to a depth of 5.0 m, we analyzed the water migration mechanism in the heterothermozone (subsurface zone of variable temperature). The results show that, from March to November, the temperature and absolute humidity (AH) increase. This is due to the flow of solar heat entering the soil — the soil subsequently releases moisture and the soil is in a state of increasing AH so that evaporation occurs. From November to March, the temperature decreases. Now, the soil absorbs water vapor and AH is in a state of decline. Thus, it is temperature alternation in the heterothermozone — due to solar heat transfer — that provides the main driving power for PE. When it drives water vapor to move downwards in the heterothermozone,

* Corresponding author: The Conservation Institute of Dunhuang Academy, Dunhuang, 736200, Gansu, China.
Tel.: +86-135-19371629; Fax: +86-937-8869103; E-mail address: dhlhs69@163.com

a small part is reversed upwards and evaporates. Solar radiation intensity dominates the annual sinusoidal PE characteristics.

Keywords: mechanism; phreatic water; heterothermozone; Mogao Grottoes

1. Introduction

Lack of water is the primary cause of land deterioration (Zhou et al., 2007). In a typical hyper-arid area, not only is the climate dry but the water table depth of phreatic water (PW) is usually deeper than the capacity of the capillary action in operation (Chen and Qi, 2004; Lehmann and Or, 2009; Tan et al., 2014). This forms extremely dry soil. The soil water content is far below the wilting coefficient. It is generally not enough to keep plants alive (Zencith et al., 2002), and this leads to a lack of vegetation. Due to this lack of vegetative protection, hyper-arid zones usually coincide with the most serious land deterioration (Ci and Yang, 2010).

To find available water resources is the first and most importance thing and is key to ecological recovery. Currently, it is not practicable to improve the ecological environment in a hyper-arid zone by changing the arid climate. Thus, we have no alternative but to look for groundwater (Braune and Xu, 2010). However, for a long time it was commonly believed that with an increase in depth-to-groundwater, there would, at some point, be no PW available (Shah et al., 2007). Gardner and Fireman (1958) initially raised the concept of ‘extinction depth’ or ‘maximum depth’ — for a water table at a level below this extinction depth the phreatic evaporation (PE) would be zero.

Generally, it was also thought that the moisture in soil in hyper-arid areas is the residue from rainfall (Warner, 2008). In arid areas, temperature changes lead to the soil moisture undergoing obvious fluctuations (Rose, 1968a, 1968b; Philip and de Vries, 1957; Scanlon, 1994). For

extremely arid areas with more intense solar radiation and severe temperature changes, the present authors do not consider the concept of extinction depth to be appropriate. Instead, it is our belief that PW is the main water source in the soil in such hyper-arid areas. We contend that PW vapor can penetrate through such thick soil layers and form evaporation (Li et al., 2010a).

To support our propositions, we designed a closed greenhouse system. Inside, an air-conditioner was installed in order to counteract the warming effect of the greenhouse. The air-conditioner used was also able to condense water to reduce the air humidity which again made the conditions inside the greenhouse closer to those outside. At the same time, the condensed water could be used to measure the quantity of PE occurring. After 45 days of monitoring it was found that there had been 0.0219 mm d^{-1} of PE (Li et al., 2010b). In addition, the daily amount of evaporation had the characteristic appearance of a sinusoidal curve (Li et al., 2014a).

However, the 45-day air-conditioner experiment had some unfortunate shortcomings. Firstly, the air-conditioner did not completely restrain the increase in temperature and humidity in the greenhouse. This was because its power was unfortunately too small and so there was still some further restraining required (Li et al., 2010b). Secondly, 45 days of monitoring is too short a time to be indicative of the *annual* PE cycle. Thirdly, our analysis of the evaporation mechanism was based only on monitoring of the daily temperature and humidity of shallow soil at 0–60 cm depth (Li et al., 2010b; 2014a). Thus, the mechanism responsible for water vapor passing through deeper layers could not be probed.

The determination of how the basic quantity of PE varies (and the mechanisms involved) on a larger spatial and temporal scale (this time tests PE for 6 years and monitoring annual soil temperature and humidity to a depth of 5.0 m) clearly has very important scientific value with respect to recovering vegetation on desertified land and for evaluating the PW resources in

hyper-arid areas. Thus, further experiments were carried out.

2. Materials and methods

2.1 Study area

The Gobi location for the condensing-air-conditioner greenhouse experiments lies at the top of the Mogao Grottoes (40°02'14' N, 94°47'38' E). It is about 1 km from a group of caves and 40 m from the greenhouse used in the 45-day experiment (Fig. 1). In this area, the depth of the buried PW is over 200 m (Li et al., 2010a). Three observation holes, each deeper than 150 m, were dug to investigate the geological and water conditions near our research site during 2007−2008. No seepage water was detected, and the soil water content was only 1.0−1.5% (mass percent, the same measure is used from this point on). Therefore, there was no capillary water present. The water present in the soil consisted of bound water, e.g. hygroscopic water, film water, and water of crystallization. The soil salinity was about 0.5−1.5% (Guo, 2009). The strata can be divided into three series: the lower Pleistocene series (Yumen group, Q_1), mid-Pleistocene series (Jiuquan group, Q_2), and the upper Pleistocene series (Gobi group Q_3). The upper 4 m of the Gobi soil is loose gravel sand, and the lower layer consists of conglomerates; the porosity is 15−30%. The top 50 cm of the soil has high salinity (4.4% on average), and mainly consists of Na_2SO_4 and NaC1. The water in the soil is mainly present as water of crystallization, e.g. $Na_2SO_4 \cdot 10H_2O$. The soil water content lies in the range 2.0–9.0% and fluctuates with the daily temperature (Li et al., 2010a; 2014a).

Here is Fig. 1

The climate is extremely dry; the annual relative humidity (RH) is 31% and there is no dew

whatsoever throughout the year. The annual precipitation is 42.2 mm and 85% of the precipitation events involve less than 5 mm — precipitation of more than 10 mm usually occurs not more than once per year. The intensity of the solar radiation can reach 1.1 kW m^{-2}, the sunshine rate is 71%, and the mean temperature is 11.23 °C. The average wind speed is 4.1 m s^{-1} (Li et al., 2010a). The potential evaporation is 4,348 mm (Guo, 2009).

Precipitation is the most sensitive factor in this experiment. According to the weather station at the top of Mogao Grottoes, the total annual precipitation was only 8.2, 26.7, and 11.19 mm in the years 2008–10. The precipitation events 2010 amounted to 2.79, 0.25, 1.80, 3.05, 0.25, 0.51, 1.27, and 1.27 mm (March 3, 5 and 7, April 9, 10, 20 and 24, and May 4, respectively). These occurred before the greenhouse was built (on May 16, 2010). According to a calculation based on simulated precipitation experiments (Li et al., 2010a), all rainfall had completely evaporated by May 10, i.e. before the greenhouse was built. From 2010 to 2015, the annual precipitation was 25.63, 56.40, 32.52, 38.10, 28.50, 40.50 mm, respectively.

2.2 Methods

2.2.1 Greenhouse–air-conditioner system

A hemispherical greenhouse was built using PVC film on a preselected site on top of Mogao Grottoes (Fig. 1). Its height was 1.8 m and radius 3.1 m, giving an area of 30 m^2 and volume of 30 m^3. The film's edge was buried 30 cm into the soil, deeper than the depth generally affected by rainfall. A 5 kW Gree air-conditioner [KFR-120 LW (12568L) AL-HN5], was installed in the greenhouse to make the temperature and humidity in the greenhouse comparable to that of the outside environment (note the much greater power of this device compared to the 2 kW air-conditioner used in 2009). The air-conditioning temperature was set at 16 °C and the unit was used in automatic mode. An air-conditioning condensation drain was used to discharge the condensed water to a sealed plastic bag outside the greenhouse. A scale was used every day (at

8:30 a.m.) from 2010 to 2015 to weigh the condensed water. The condensed water recorded was taken to be equal to the amount of PE.

2.2.2 Temperature and humidity monitoring in the greenhouse

Two temperature and humidity mini-monitors (HOBO-U23-001, USA) were installed in the greenhouse. One was 50 cm above the ground and one 30 cm underground (after 2011, this was changed to 40 cm and another monitor was added at 60 cm). The recorded temperatures were accurate to ±0.7 °C from –40 to 100 °C, and ±0.18 °C from 0 to 50 °C. The RH measurements were accurate to ±2.5% from 10% to 90% and ±4.0% from 0% to 10% and 90% to 100%. Two identical devices were also laid outside the greenhouse in the same way.

The mini-monitors recorded the changes in the air temperature and humidity inside and outside the soil every 10 min. The soil water content was also monitored at depths of 10, 20, 30, 40, 50, and 60 cm, sampling in 1 cm thickness in different stages. After considering the daily temperature effects (Li et al., 2010a), the soil was sampled at 9:30 a.m. using a method of weighing and oven drying. A comparison was made to analyze the changes in the soil humidity after long-term water output. The general idea was that if the soil moisture did not decline then we would know that the water of evaporation was not coming from rainwater stored in the soil, and that there must be a channel and mechanism for PW to move upwards.

2.2.3 Temperature and humidity monitoring at 5-m depth

In relation to PE, it is still a key focus at present to determine whether or not the evaporated water collected by the air-conditioner comes from PW (and, therefore, whether the existence of a migration mechanism is the key to judging the source of PW). Prior to this study, migration mechanisms were analyzed based mainly on the daily temperature and humidity of shallow soil at 0–60 cm (Li et al., 2010a; 2014a). The current experiment also adopted this method, but with

one difference — a 5-m deep pit was dug outside the greenhouse. In this pit, 10 temperature and humidity monitoring instruments (HOBO-U23-001) were buried underground at progressively greater depths (with 50 cm between consecutive devices). Then, the pit was backfilled. Using a recording interval of 30 min, these instruments were used to 'continuously' monitor the yearly temperature and humidity. According to the monitoring records we could thus analyze the migration mechanism of PW on a larger spatio-temporal scale.

3. Results

3.1 Quantity of PE

Except for just over half a year in 2013, during which we stopped collecting PE, the monitoring process recorded the collection of 577.719 kg of evaporated water from the greenhouse in total. The collection data is presented in detail in Fig. 2.

Here is Fig. 2

From May 17, 2010 to August 25, 2015, the yearly amount of collected PE was 115.111, 101.703, 121.511, 20.450, 133.645, and ~~85.299~~114.157 kg, respectively. For two of the years, 2012 and 2014, the PE was monitored for the entire year (Fig. 2b). According to the PE measured over 2010–15 to calculate the same period of average evaporation, and then obtain the average annual PE is 4.52 mm (Fig. 2c). The PE has a sinusoidal trend, which is similar to the daily evaporation (Li et al., 2014a). The PE changes with the change in temperature over the year, increasing with the temperature rise in spring and decreasing in the fall (Fig. 2b and 2c).

The evaporation period lasts from March to November — at other times there is no PE. Even within this band, there are several days every year with zero PE, as can be seen in Fig. 2. This is mostly due to cloud cover (a few days can be attributed to power failure).

It must be pointed out that a rainfall event of 48.8 mm was encountered on June 16, 2011. This corresponds to the most rainfall (in 24 hours) recorded in the Dunhuang region since 1938. The authors thought that this was a good opportunity to observe the effect of heavy precipitation on PE (any effects should be very obvious). However, our results show that the PE remained relatively stable — there were no sudden increases (Fig. 2a), even though the soil humidity outside was far greater than that in the greenhouse after the precipitation. For example, in 2010, 2011, 2012, 2014, and 2015, the average PE was ~~833~~614, ~~897~~667, ~~747~~553, ~~902~~671, and ~~830~~ 647 g d^{-1} for the same period (June 20 to ~~August~~ October ~~25~~26), respectively~~,~~. Compared with this PE of 2010, ~~with a~~the fluctuation amplitude ~~of~~was 8.7%, –9.9%, 9.3% and 5.4%, respectively in 2011, 2012, 2014, and 2015 ~~less than 7%~~. This also suggests that the evaporating water is not from rainfall residue. If the evaporating water is residual rainfall, then the PE in the greenhouse should decline gradually with rainwater evaporation, so the PE in the same period (June 20 to August 25) should decline gradually from 2010 to 2015. However, the results indicate that this is not the case.

It is also worth noting that the average quantity of PE recorded (827 g d^{-1}) is 25.9% larger than that recorded during the 45-day experiment in 2009 (Li et al., 2010b) for the same period (May 22 to July 5). This is because of the greater power of the new air-conditioner.

3.2 Change in soil water content

The data for the soil water content inside and outside the greenhouse recorded in the different years is shown in Fig. 3.

Here is Fig. 3

If the evaporated water came from residual rainfall, then the soil water content would also

show an obvious decrease (about 1.6%) after ~~578–~~607 kg of water had evaporated in the greenhouse. However, this was not the case. The average water content of the soil in the 0–60 cm layer in the greenhouse changed in the range 3.16–4.33%, and even at the late stage (4.33%) exceeded the initial value (3.46%, May 19, 2010). This demonstrates that the soil water content was fluctuating on a daily basis (Li et al., 2010a) and the evaporating water was supplied by the subsoil. However, although the evaporating water comes directly from the subsoil, in the long run, it comes from PW.

3.3 Comparison of temperature and humidity inside and outside the greenhouse

A comparison of the temperature, RH, and absolute humidity (AH) measured inside and outside the greenhouse in 2010 is shown in Table 1.

Here is Table 1

The mean temperature, RH, and AH 50 cm above the ground inside the greenhouse were all lower than those of the outside (by 2.35 °C, 1.21%, and 0.94 g m^{-3}, respectively). At 30 cm under the ground, the inside values were again ~~lower~~lowers than those outside (by 0.79 °C, 1.38%, and 1.57 g m^{-3}, respectively). This shows that the air-conditioner effectively restrained the influence of the greenhouse effect on the temperature and humidity (and made them slightly lower than the atmospheric values). Thus, the evaporation measured this time should already have reached the actual evaporation quantity.

As the outside temperature and humidity at –30 cm were higher than those inside the greenhouse, we think that there was probably a small amount of moisture from the outside soil entering into the greenhouse. The temperature and humidity monitoring data at 5-m depth shows that the RH of the external soil rose rapidly to 100% after 48.8-mm precipitation. Below 30 cm it

stayed at 100% from June 20, 2011 to 2015, whereas, in the greenhouse, the RH at 30, 40, and 60 cm remained stable at 66%, 73%, and 84%, respectively, which is consistent with the values before the precipitation. Sketches illustrating this are shown in Fig. 4.

Here is Fig. 4

After precipitation, the RH of the soil obviously increases. However, the PE (Fig. 2) did not increase significantly all the way from 2011 to 2015 [PE was not consistently higher than the PE in 2010; the PE was 553 g d^{-1} in 2012 ~~(747 g d^{-1}) and 2015 (830 g d^{-1}) were~~ even lower than that in 2010 (~~833~~ 614 g d^{-1})]. This suggests that different soil RH values outside have very little influence on PE. There was almost no water vapor flowing horizontally into the greenhouse soil (Fig. 4b). The influence is less than the influence of confounding climate factors, such as, the yearly temperature (±1 °C), sunshine rate (±3%), etc.

If we just consider the results from the outside soil humidity monitor by itself, then the heavy precipitation event (Fig. 3, b–f; Fig. 4b) gives us plenty of reasons to think that the soil water is the residue of the rainfall. After heavy precipitation, rainwater infiltrates into the deep soil. Then, due to evaporation, the ground surface forms a dry layer, which strongly restrains evaporation. Hence, the rainwater will be preserved for a long time in the sub-layer. But systematic experiments have proved that this is not the case.

We have performed systematic experiments to exclude rainwater. A rainfall simulation experiment showed that 5, 10, and 16 mm of rainfall evaporated completely after 8, 12, and 23 days, respectively (Li et al., 2010a). An isolated experiment using a 200 cm × 200 cm × 200 cm pit likewise manifested that even 25 mm of rainfall could evaporate fully within one year (Li et al., 2013). An experimental simulation on take-back of 5-mm rainfall proved that the rainfall did

not enter into the soil as vapor form — 5 mm of rainfall can be completely taken-back by the greenhouse–air-conditioner method (Li et al., 2014b). Furthermore, the soil moisture remained elevated at depths of 10 to 20 cm for 3 years, which is similar to what happened with the outside soil water content after this 48.8 mm precipitation event (Fig. 3b–f). The rainfall reduced the soil's hydrophobicity and the elevated soil moisture causes PE to increase thereafter. This shows that, in a normal year, the rainfall just evaporates completely (i.e. the yearly evaporation capacity is greater than the rainfall received). Even this once-in-a-century amount of rainfall should have completely evaporated by the end of 2017, according to the experimental data (in the first year the evaporated rainwater was more than 25 mm, then $4.52 \times 6 = 27.1$ mm from 2012 to 2017, which is a greater total amount than the 48.8 mm precipitated). Therefore, if the PE in greenhouse was mainly supported by the outside 48.8 mm rainfall, the amount of PE should decrease sharply in 2015, but in practice this was not the case, so there must be a PW source in this extremely arid area. The 4.52 mm yr^{-1} evaporation rate corresponds to the background PE rate in this area.

3.4 Temperature, humidity, and the water-movement mechanism in the heterothermozone

The air temperature and humidity monitoring results at 50–500 cm depth in 2010, the representative of a 'normal' year, are shown in Fig. 5. The soil temperature and AH change with the annual revolution of the Earth. Fig. 5 reflects the basic annual changes in the heterothermozone.

Here is Fig. 5

From November to March 2010, both the temperature (Fig. 5a) and AH (Fig. 5c) in the soil increased gradually from shallow to deeper layers. For the bound water in the hyper-arid soil, the

basic behavior is that when the temperature is rising, the combined water gradually decomposes so vapor is released. When the temperature drops, the soil absorbs moisture. Meanwhile, according to the vapor migration rule, moisture migrates from areas with high temperature and high humidity to areas with low temperature and low humidity. The higher temperature and vapor concentration (AH) in the deep layers provide sufficient conditions to make moisture move upwards. So, at these times, water vapor certainly migrates upwards. The distribution of temperature and humidity has an approximately opposite situation from March to November, so that water vapor essentially moves downwards. A more detailed account of the mechanism driving the yearly water movement in the heterothermozone is as follows.

At the beginning of February, the water vapor migrates upwards and most of the water vapor transforms to soil-bound water, i.e. hygroscopic water, film water, and water of crystallization. The whole of the upper heterothermozone is in a vapor density declining and absorbing state. Therefore, there is no evaporation.

However, viewed in terms of the spatial variation in temperature in a sequence of soil layers (from shallow layers to deeper ones), it changes in an orderly fashion and there are also delays. The deeper parts suffer more serious temperature delays. In Fig. 5a, the temperature begins to increase in the 50 cm soil from February onwards. At that time, due to the higher temperature and AH in the subsoil, the evaporated water did not enter into the subsoil. Instead, it flowed into the upper soil and was absorbed. As the temperature gradually increased, from March onwards, the upper soil could not absorb all the vapor, and so the real evaporation (i.e. PE) began and also gradually increased (Fig. 2).

At the end of May, the whole temperature distribution in the 5 m layer began to reverse, i.e. the shallower layers became warmer than the deeper layers. The AH distribution followed the

same pattern (Fig. 5c). At this time, according to the moisture migration rule, water vapor in the upper soil should largely move to lower levels. However, because the transportation capability of the available passages (i.e. pores in the soil) was not enough to transport the quantity of the water decomposing, a part of the vapor was reversed upwards and formed evaporation. Thus, the PE increased to a higher level.

The temperature in the 50 cm deep soil began to decrease in August. While the temperature is decreasing, the soil will rapidly absorb water to recover water content. This behavior is just the opposite of bound water passing into the vapor state as temperature increases. Where the soil is still experiencing increasing temperature (due to the temperature delay in the subsoil), the bound water will continue to transform into vapor. Most of the water vapor will still migrate down into the subsoil where the soil has lower temperature and lower humidity, but a small quantity of the vapor still reverses upwards. This 'reversed vapor' meets and exceeds the amount of absorption occurring in the upper soil, so a small part penetrates the buried layer and evaporates. The PE then gradually declines.

As the temperature increasing layer becomes deeper, and the amplitude of its temperature increase declines, the amount of upward-moving water vapor becomes smaller. After November, the soil absorbs all of the decomposed water vapor and recovers its soil water content to prepare for evaporation in the next year. There is no overflow of water vapor to the ground surface and no evaporation.

Therefore, from March to November, in the temperature reversing stage, the whole of the upper heterothermozone is in a state of water vapor pressure 'expansion'. This forms stronger evaporation and the soil loses water. From November to March of the next year it is in a state of water vapor pressure 'contraction' wherein the soil absorbs humidity and recovers water content.

Viewed as a yearly evaporation process, PE follows a sorption/desorption model in which it is influenced by temperature, the 'power pump' for the PE. Thus, the PW in hyper-arid areas migrates from lower to upper parts year after year and forms evaporation.

In summary, in the upper half of the heterothermozone, the time over which the main upward/downward moisture migration occurs is approximately six months in each year. The sum of the PE quantity and downwards moving water balances the amount moving upwards. The PE (4.52 mm yr^{-1}) accounts for a very small part of the yearly moisture fluctuation in the whole of the heterothermozone.

The depth of the stratum influenced by annual temperature changes, i.e. the heterothermozone, is generally 20–30 m (Liu and Cai, 2000). In the deeper layers below the heterothermozone the temperature gradient increases 4 °C per hectometer due to geothermal effects (Li et al, 2011). Below 3.0 m the RH is kept in a state of saturation (Fig. 5b), so AH rises with increasing depth. Thus, deeper layers have high temperature and AH encouraging water vapor to continuously move upwards. There are stable conditions for water vapor to be continuously converted to film water. Film water is bound water and is not affected by gravity. It can slowly move, however, from areas of high hydraulic potential to areas of lower hydraulic potential. Condensation makes the film water thicker in the deeper soil. The upper layer's film water is relatively thin because of evaporation. So, film water will move upwards. At the same time, the film water can dissolve a small amount of mineral salts. With long-term water evaporation, a large quantity of salts is detained in the shallow soil layers and forms a salt-rich stratum in hyper-arid areas. This is an important feature of arid land and is also strong evidence for the existence of upward moving film water. Therefore, in hyper-arid areas, apart from a PW-vapor moving form, film water is another important form of PW movement.

Thus, PW is a major source of soil water in hyper-arid areas and supports the survival of drought-tolerant plants. A better understanding of the annual characteristics of PE in hyper-arid areas is therefore very important for ecological rehabilitation.

4. Discussion

4.1 Interaction between the daily and yearly heterothermozones

The evaporative interface is in the 'daily heterothermozone' region 0–60 cm. In addition to a small amount of water evaporating during the daytime, most of the soil moisture flows into the subsoil layer (the 'yearly heterothermozone' region) because of the strong driving force of the solar radiation (temperature). At night, this subsoil moisture migrates upwards and restores the soil's water content due to the subsoil's higher temperature and humidity (Li *et al*., 2014a). Water movement from 0 to 60 cm in the day-time is analogous to the yearly heterothermozone during March to November; at night, it is similar to the yearly heterothermozone in winter. The PE has the fractal structure's self similarity characteristics on daily and yearly scale.

However, the soil's water content in the daily heterothermozone alone is not enough if there is no water replenishment and support from the yearly heterothermozone — the evaporation would be unsustainable. Therefore, on a yearly scale, the evaporation characteristics are controlled by the annual temperature changes in the heterothermozone. In nature, it is the solar heat energy that flows into the soil that makes the water evaporate. The continuous flowing and orderly transfer of temperature (heat flow) in the heterothermozone is the major dynamic source of PE and governs the form of its yearly characteristics. Solar radiation is the driving power underlying PE.

On the whole, deeply-buried PW forms an orderly continuum with an orderly and continuous mode of operation from bottom to top. Hypothetically, if there were no inherent geothermal heat-

driving effects, the PE would be smaller. If there were no yearly/daily solar radiation cycles (i.e. temperature fluctuations), then there would also be a stable but smaller continuous movement and evaporation under geothermal action. In other words, it is the change in temperature on a yearly/daily basis that alters the stable evaporation character and forms a sinusoidal variation. The soil is both the 'source' and the 'sink' for soil water, and the water vapor moves over short distances. The transformation of bound water, under the effect of temperature, to water vapor in the heterothermozone plays an important role in the moving up of PW. Most of the soil water migrates up and down along with the changes in the temperature field in the soil. This analysis is similar to one given by Scanlon (1994) in the Chihuahuan desert. The quantity 4.52 mm yr^{-1} for PE rate is consistent with Ambroggi (1966) who estimated 3.0 mm yr^{-1} in the Sahara, where the burial depth of the water is 20 m.

4.2 Relationship between the amount of PE and soil-water hysteresis

In addition to temperature, the basis of the soil water content plays a key role in the evaporation quantity. Extremely dry soil exhibits a soil-water hysteresis phenomenon (Hopmans and Dane 1986). If the basis of the soil water content is different for the same temperature change (as they are in the main wetting and drying curves), the water content will vary with different amplitudes. In an environment with a certain humidity, this can restore water content (Qian and Liu, 2007; McNamara, 2014). This is just the situation in the 0–60 cm layer of the soil in the greenhouse, and is why the water content maintains certain fluctuations (Fig. 3). The daily temperature of the continuous cycle fluctuation forms the evaporation. So, when the basis of the soil water is at a 'constant value' such as in the greenhouse, the evaporated water quantity is related to the change in temperature. This explains why, after the heavy precipitation event, the greenhouse's PE remained stable in 2012–15. The amplitude of the fluctuation in PE ~~(7%)~~ was

mainly affected by the yearly climatic temperature variation.

Rainwater infiltration and redistribution can increase the moisture in the deep soil (including RH). But, after water evaporation and diffusion, the free rainwater quickly turns into bound water. However, such bound water cannot be transformed into water vapor for more than half of the year (in the temperature declining or stable period). Therefore, even if there is a certain RH/AH in the greenhouse soil that is higher than outside's (Fig. 4b), then there is no water vapor flowing into the greenhouse as the soil cannot indeed provide water vapor. Thus, such an RH gradient is a kind of 'imitation' gradient compared to the wet soil case in which there is, at least, hanging water available. The current formulae used to calculate vapor flow in unsaturated soil, e.g. the Fickian diffusion law (Philip and de Vries, 1957) and others (Rose, 1968a, 1968b; Shokri et al, 2010; Scanlon and Milly, 1994; Tan et al., 2014) were derived for use with relatively wet soil (compared to hyper-arid soil). Unlike hyper-arid soil (in which we must consider the control the varying temperature has over the quantity of water vapor), 'wet' soil can provide sufficient water vapor without considering the vapor quantity of soil provided: in the case of constant temperature, moisture migration is always present in the wet soil, as long as there is an air humidity gradient. So, whether or not these formulae are appropriate for extra-arid soil needs further discussion.

4.3 PE and 'extinction depth'

For shallow water tables, the soil does at least contain capillary water. Therefore, PE is high. The concept of 'extinction depth' (Gardner and Fireman, 1958), wherein the PE declines sharply when the burial depth of the water reaches the maximum height of the rising capillary water, was proposed based on such high PE levels. We measured a PE quantity of 4.52 mm yr^{-1} in a typical hyper-arid area which is larger, relatively, compared with that required for the survival of

drought-tolerant vegetation. However, compared to PE supported by a continuous supply of capillary water, it can be ignored. The two amounts have entirely different orders of magnitude. Therefore, 'extinction depth' is a relative concept (Shokri and Salvucci, 2011).

5. Conclusions

After monitoring PE for 6 years in a hyper-arid area, we determined the basic characteristics and quantity of PE on a yearly scale. The PE has sinusoidal characteristics and changes along with the soil's yearly temperature variation. The annual evaporation is 4.52 mm. Accordingly, our analysis of the monitored temperatures and humidity in soil at depths of 50–500 cm shows that there exist conditions and migration mechanisms for PW in the heterothermozone and deeper soil. Due to the effect of temperature, moisture in the heterothermozone moves orderly in space and time. Geothermal forces also have an important effect on PE. It is clear that PW is a new and important water resource available to effect ecological rehabilitation in hyper-arid areas.

Acknowledgments

We gratefully acknowledge funding from the National Natural Science Foundation of China (No. 41363009), the Dunhuang Academy (No. 201306), and the Gansu Province science and technology plan (No. 1308RJZF290).

References

Ambroggi, R.: Water under the Sahara, Sci. Am., 214, 21–29, 1966.

Braune, E. and Xu, Y.: The role of ground water in sub-Saharan Africa, Groundwater, 48, 229–238, 2010.

Chen, X. and Qi., H.: Groundwater influences on soil moisture and surface evaporation, J.

Hydrol., 297, 285–300, 2004.

Ci, L. J. and Yang, X. H.: Desertification and its Control in China, Higher Education Press, Beijing, 9–27, 2010.

Gardner, W. R. and Fireman, M.: Laboratory studies of evaporation from soil columns in the presence of a water-table, Soil Sci., 85, 244–249, 1958.

Guo, Q. L.: Origin of Water and Salts Responsible for Wall Paintings Disease at Dunhuang Mogao Grottoes, Lanzhou University, Lanzhou, 2009.

Hopmans, J. W. and Dane, J. H.: Combined e_ect of hysteresis and temperature on soil-water movement, J. Hydrol., 83, 161–171, 1986.

Lehmann, P. and Or, D.: Evaporation and capillary coupling across vertical textural contrasts in porous media, Phys. Rev. E, 80, 046318, doi:10.1103/PhysRevE.80.046318, 2009.

Li, H. S., Wang, W. F., Zhan, H. T., Qiu, F., and An, L. Z.: New judgement on the source of soil water in extremely dry zone, Acta Ecologica Sinica, 30, 1–7, 2010a.

Li, H. S., Wang, W. F., Zhang, G. B., and Zhao. L. Y.: Measurement of deep buried phreatic water evaporation in extremely arid area, Acta Ecologica Sinica, 30, 6798–6803, 2010b (in Chinese).

Li, H. S., Wang, W. F., Zhang, G. B., Zhang, Z. M., and Wang, X. W.: GSPAC water movement by greenhouse method in the extremely dry area, Journal of Arid Land, 3, 141–149, 2011.

Li, H. S., Wang, W. F., Liu, B. L., Zhan, H. T., and Qiu, F.: Applying isolation method study soil water source in the extreme dry area, Arid Land Geography, 36, 92–100, 2013 (in Chinese).

Li, H. S., Wang, W. F., and Liu, B. L.: The daily evaporation characteristics of deeply buried phreatic water in an extremely arid region, J. Hydrol., 514, 172–179, 2014a.

Li, H. S., Wang, W. F., Zhan, H. T., and Zhang, G. B.: Application of a greenhouse airconditioning method to simulate take-back of rainfall in an extremely arid area, Acta Ecologica Sinica, 34, 6182–6198, 2014b.

Liu, B. P. and Cai, Y. L.: An Introduction to Earth Science, Higher Education Press, Beijing, 78–79, 2000.

McNamara, H.: An estimate of energy dissipation due to soil-moisture hysteresis, Water Resour. Res., 50, 725–735, 2014.

Philip, J. R. and de Vries, D. A.: Moisture movement in porous materials under temperature gradients, T. Am. Geophys. Un., 38, 222–232, 1957.

Rose, C.: Water transport in soil with a daily temperature wave, I. Theory and experiment, Aust. J. Soil Res., 6, 31–44, 1968a.

Rose, C.: Water transport in soil with a daily temperature wave, II. Analysis, Aust. J. Soil Res., 6, 45–57, 1968b.

Scanlon, B. R.: Water and heat fluxes in desert soils: 1. Field studies, Water Resour. Rese., 30, 709–719, 1994.

Scanlon, B. R. and Milly., P. C. D.: Water and heat fluxes in desert soils: 2. Numerical simulations, Water Resour. Res., 30, 721–733, 1994.

Shah, N., Nachabe, M., and Ross, M.: Extinction depth and evapotranspiration from ground water under selected land covers, Groundwater, 45, 329–338, 2007.

Shokri, N. and Salvucci, G. D.: Evaporation from porous media in the presence of a water table, Vadose Zone J., 10, 1309–1318, 2011.

Shokri, N., Lehmann, P., and Or, D.: Liquid-phase continuity and solute concentration dynamics during vaporation from porous media: pore-scale processes near vaporization surface, Phys.

Rev. E, 81, 046308, doi:10.1103/PhysRevE.81.046308, 2010.

Tan, X. C., Wu, J. W., Cai, S. Y., and Yang, J. Z.: Characteristics of groundwater recharge on the North China Plain, Groundwater, 52, 798–807, 2014.

Qian, T. W. and Liu, C. G.: Migration of Pollutant in Saturated-Unsaturated Soil, China Environmental Science Beijing press, Beijing, 28–26, 2007.

Warner, T. T.: Desert Meteorology, China Meteorological Press, Beijing, 136–151, 2008 (translated by Wei, W. S., Cui, C. X., and Shang, H. M.).

Zhou, A. G., Sun, Z. Y., and Ma, R.: Geo-ecology in Arid Regions: an Introduction, Higher Education Press, Beijing, 46–52, 2007.

Table 1. Comparison of average temperature (in °C), relative humidity (RH in %), and absolute humidity (AH in g m^{-3}) inside and outside the greenhouse for the year 2010.

Position (cm)	Temperature (°C)		RH (%)		AH (g m^{-3})	
	Inside	Outside	Inside	Outside	Inside	Outside
+50	19.35	21.70	29.00	30.21	4.83	5.77
–30	22.95	23.74	66.4	70.78	13.61	15.18

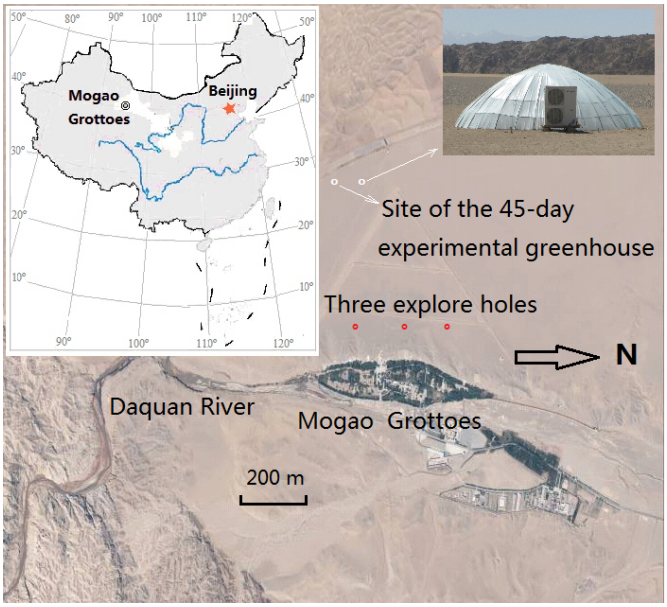

Fig. 1. The site of the experiment and the greenhouse/air-conditioner system.

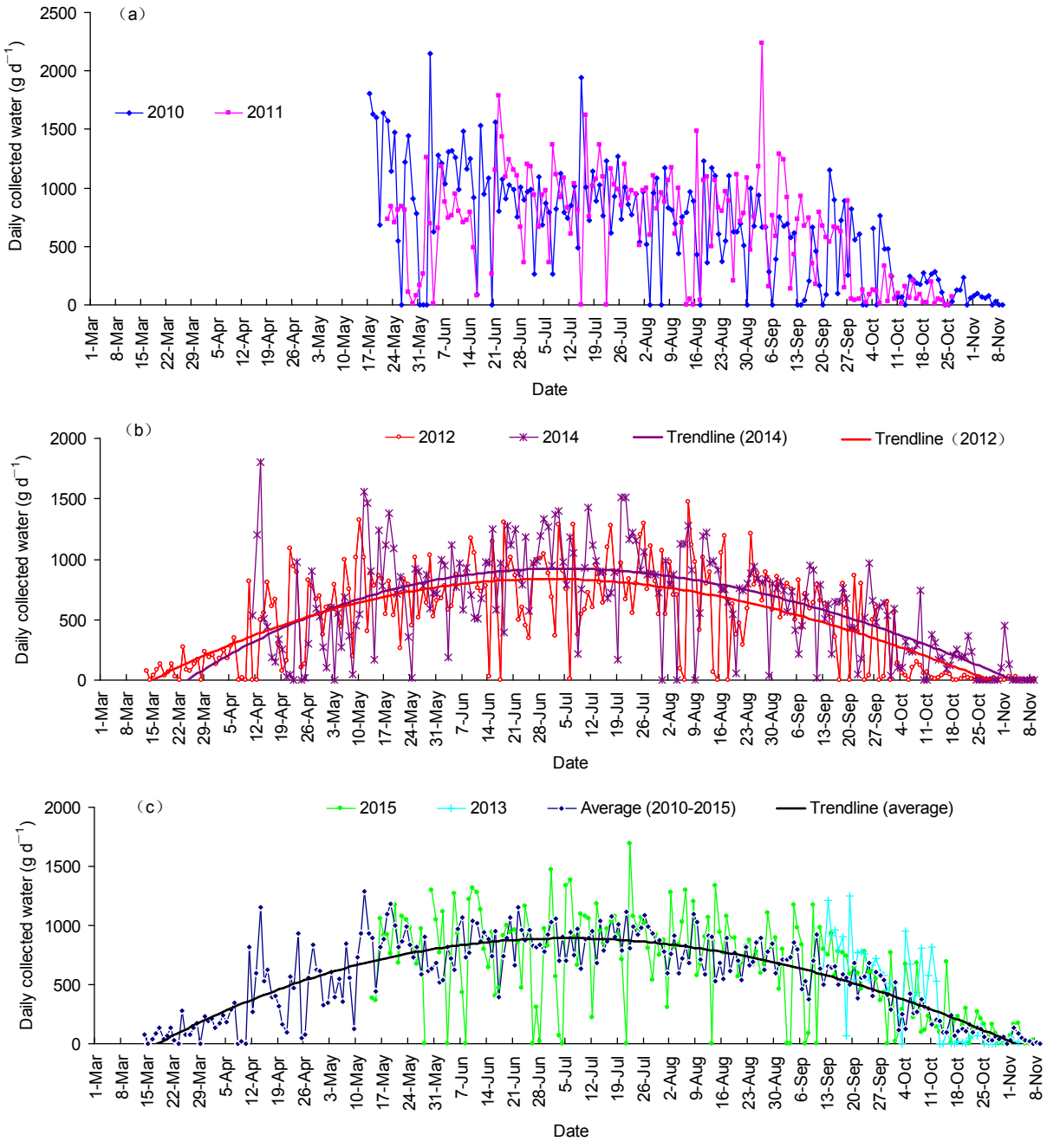

480

Fig. 2. The quantity of water collected from the greenhouse from 2010 to 2015. (a) Refers to the collected water in 2010 and 2011, (b) the collected water and trendlines in 2012 and 2014, and (c) the average trendline and collected water in 2013 and 2015.

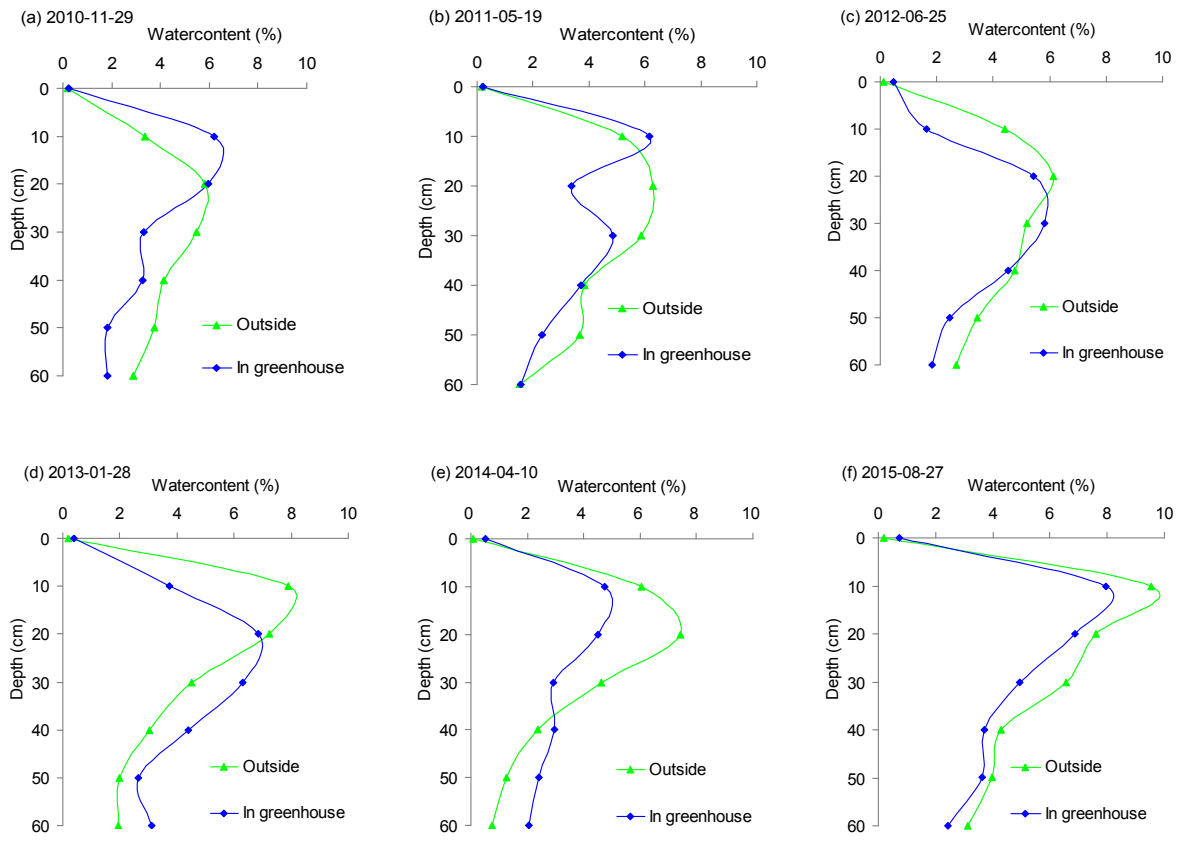

Fig. 3. Soil water content inside and outside the greenhouse in the different stages. (a) Represents soil water content of beginning, (b) the earlier stage in spring, (c) the middle stage in spring, (d) the middle stage in winter, (e) the late stage in spring, and (f) the late stage in summer.

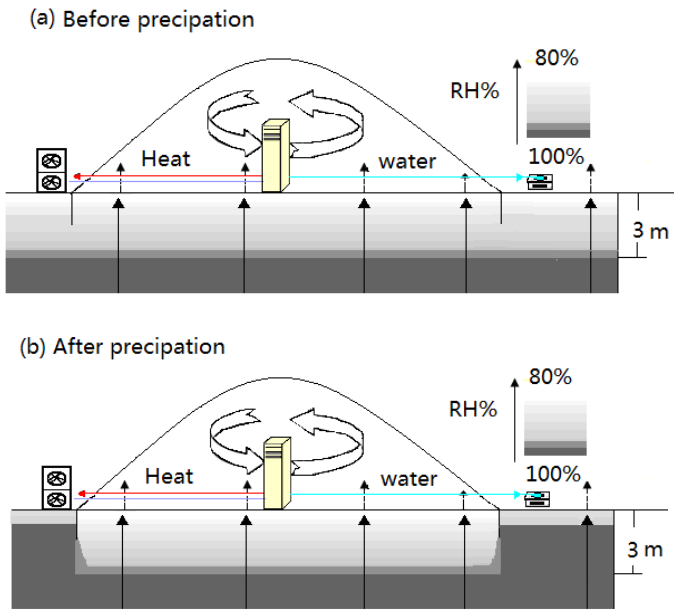

Fig. 4. The air humidity profiles before (a) and after precipitation (b).

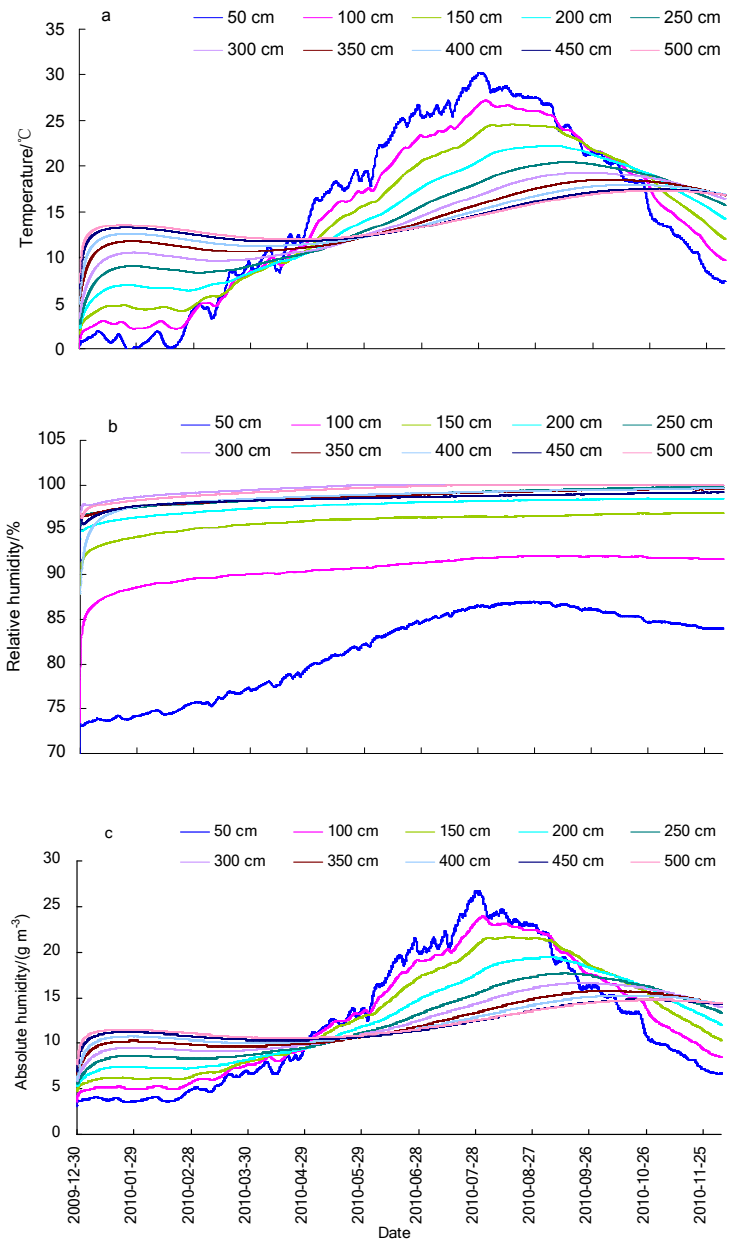

495 **Fig. 5.** The yearly change in (a) temperature (in °C), (b) relative humidity (RH in %), and (c) absolute humidity (AH in g m^{-3}) in 500 cm of soil.